C. R. Palevol 16 (2017) 645–654

Contents lists available at ScienceDirect

Comptes Rendus Palevol

www.sciencedirect.com

Human Palaeontology and Prehistory

Morphological correlates of the first metacarpal proximal articular surface with manipulative capabilities in apes, humans and South African early hominins

Corrélations morphologiques de la surface articulaire proximale du premier métacarpe avec les capacités de manipulation chez les grands singes, les humains et les hominines archaïques sud-africains

Damiano Marchi[a,b,*], Daniel J. Proctor[c], Emma Huston[c], Christina L. Nicholas[d], Florian Fischer[e]

[a] *Dipartimento di Biologia, University of Pisa, Pisa, Italy*
[b] *University of the Witwatersrand, Johannesburg, South Africa*
[c] *Department of Anthropology, Lawrence University, Appleton, USA*
[d] *Dows Institute for Dental Research, The University of Iowa, Appleton, USA*
[e] *Faculty of Medicine, Ludwig Maximilian University, Munich, Germany*

ARTICLE INFO

Article history:
Received 12 July 2016
Accepted after revision 21 September 2016
Available online 10 November 2016

Handled by Roberto Macchiarelli and Clément Zanolli

Keywords:
Australopithecus africanus
Locomotion
Manipulation
3D geometric morphometrics

ABSTRACT

This study quantifies the metacarpal 1 (MC 1) proximal articular surface using three-dimensional morphometrics in extant hominids and fossil hominins (SK 84, cf. *Paranthropus robustus/Homo erectus* and StW 418, *Australopithecus africanus*) to understand which characteristics of the proximal metacarpal 1 are potentially correlated with human manipulative abilities and if they can be used in a paleoanthropological setting. A principal components (PC) analysis was used to compare MC 1 proximal articular surface shape and ANOVA and Tukey's HSD post-hoc tests were conducted to determine differences among groups. *Homo* is significantly different from nonhuman hominids having a less radioulnarly and dorsovolarly curved articular surface. All nonhuman hominids have more curved articular surface with *Gorilla* showing the most curved joint. Moreover, this study highlights the presence of a radially extended surface in *Homo* that may be related to the greater thumb abduction in human manipulation activities. Both fossils analyzed show a great ape-like MC 1 proximal articular surface which, associated with recent trabecular and archaeological evidence, may indicate that the ability to make/use stone tools preceded the morphological adaptations associated today with such behavior.

Mots clés :
Australopithecus africanus
Locomotion
Manipulation
Morphométrie géométrique 3D

RÉSUMÉ

Cette étude vise à quantifier la morphologie de la surface articulaire du métacarpe I (MC 1) en utilisant la morphométrie géométrique 3D chez les hominidés actuels et les hominines éteints (SK 84, cf. *Paranthropus robustus/Homo erectus* et StW 418, *Australopithecus africanus*), cela afin de comprendre quelles caractéristiques de la surface proximale du

* Corresponding author. Dipartimento di Biologia, University of Pisa, Pisa, Italy.
E-mail address: damiano.marchi@unipi.it (D. Marchi).

http://dx.doi.org/10.1016/j.crpv.2016.09.002
1631-0683/

métacarpe 1 sont potentiellement corrélées avec les capacités de manipulation humaines et si ces dernières peuvent être appliquées au registre paléoanthropologique. Une analyse en composantes principales (PC) a été utilisée pour comparer la conformation de la surface articulaire proximale du MC1 ; des tests post-hoc ANOVA et Tuckey HSD ont été menés afin de déterminer les différences entre les groupes. *Homo* est significativement différent des hominidés non humains par sa surface articulaire moins courbée en directions radio-ulnaire et dorso-palmaire. Tous les hominidés non humains ont une surface articulaire plus incurvée, *Gorilla* ayant l'articulation la plus incurvée. De plus, cette étude met en évidence la présence d'une surface étendue en direction radiale chez *Homo*, peut-être en relation avec le plus grand degré d'abduction du pouce humain lors des activités de manipulation. Les deux fossiles analysés montrent une surface articulaire proximale du MC1 similaire à celle des grands singes, ce qui, associé aux récents travaux sur les trabécules et aux preuves archéologiques, pourrait indiquer que la faculté de créer/manipuler des outils lithiques a précédé les adaptations morphologiques aujourd'hui associées à de tels comportements.

1. Introduction

The morphology of the hand has been prominent in anthropological studies aimed to understanding the onset of stone tool-making capabilities in early hominins (Kivell, 2015; Kivell et al., 2015; Marzke, 1997; Skinner et al., 2015). Though recent discoveries in South Africa have provided relatively complete and articulated hands for *Australopithecus sediba* (Berger et al., 2010) and *Homo naledi* (Berger et al., 2015), multiple hand bones from the same individual are rare in the fossil record. Given the importance of hand morphology to understanding early hominin behavior many studies have been devoted to developing methods for inferring hominin hand use from isolated hand bones (Almécija et al., 2010; Green and Gordon, 2008; Marzke et al., 2010; McHenry, 1983; Rolian and Gordon, 2013; Susman, 1994; Tocheri et al., 2003; Ward et al., 2014).

The human hand is mainly distinguishable from the great ape hand by a series of traits that are considered advantageous for precision-pinch grip and forceful precision grips (Marzke, 1997; Napier, 1956). It retains primitive thumb and fingers proportions, whereas the ape hand is derived in this respect (Almécija et al., 2015; Green and Gordon, 2008; Pouydebat et al., 2008; Rolian and Gordon, 2013; Susman, 1979). The extremely long, curved fingers of great apes (*Gorilla* excepted, see Almécija et al., 2015) make their hands more specialized overall than ours making manipulation more challenging relative to us (Tuttle, 1969). Otherwise, humans have many small specialized features, like a styloid process on the third metacarpal, or features of the carpometacarpal joints allowing for its versatility in use (Napier, 1955, 1956, 1960; Tocheri et al., 2008). Though great apes use their hand for manipulatory activities, their specialization is more a consequence of their locomotor behavior. However, mainly the non-pollical digits are used in great ape locomotion (knuckle-walking, suspension, fist walking), while the thumb is rarely used (Aiello and Dean, 1990; Coffing, 1998; Sarmiento, 1988; Tuttle, 1967). Further, humans use the thumb in a way different from nonhuman apes during manipulation, and it is therefore one of the regions of the hand that has been more extensively investigated to understand the anatomical correlates with the capacity to build and manipulate tools (Almécija et al., 2010; Hamrick et al., 1998; Marzke et al., 2010; McGrew, 1995; Napier, 1955; Rightmire, 1972; Susman, 1988, 1991, 1994; Tocheri et al., 2003, 2005; Trinkaus, 1989; Trinkaus and Long, 1990; Trinkaus and Villemeur, 1991).

The different use of the thumb by humans is reflected in the wide morphology of the trapeziometacarpal joint (tmcj), as compared with a smaller and both radioulnarly and dorsoplantarly more curved articulation in apes (Marzke et al., 2010; Niewoehner, 2001; Rose, 1992; Tocheri et al., 2005). More generally, the anatomy of this region of the hand in part reflects the habitual levels and directions of force transmitted through the hand (Niewoehner, 2000). The proximal joint of the first metacarpal (MC 1) has therefore been the focus of many studies aiming at quantifying the presence of signals that correlate to the different functional capabilities of the hand of extant hominids, in an effort to understand the onset of manipulatory abilities in early hominins (Lewis, 1977; Marzke et al., 2010; Niewoehner, 2000, 2001, 2005; Rose, 1992; Tocheri, 2007; Tocheri et al., 2003, 2005; Trinkaus, 1989).

Linear measurements of the tmcj cannot capture all the aspects of shape variability of this morphologically complex joint (Trinkaus, 1989). In one of the first attempt to quantify the surfaces of the tmcj, Tocheri et al. (2003) analyzed three-dimensional trapezium models from humans and great apes, as well as fossil hominins (*A. afarensis* and *H. habilis*). The authors generated least-squares planes for each articular surface and found distinct patterns distinguishing each living species from the others. In particular, *A. afarensis* showed similarities with humans suggesting the ability to perform the forceful pad-to-side and three jaw chuck grips, while *H. habilis* showed key differences with humans indicative of limitations in its functional capabilities (Tocheri et al., 2003). In another study, Tocheri et al. (2005) quantified the relative articular and nonarticular surface area of the trapezium and trapezoid of apes and humans in order to test if the differences reflected the qualitative analyses and the functional demands of the different manipulative capabilities of extant hominids. The authors found that humans are clearly distinguished from

great apes in having larger relative first metacarpal and scaphoid surfaces on the trapezium and explained it as a consequence of the regular recruitment of the thumb during manipulative behaviors (Tocheri et al., 2005).

In another study on the tmcj of Late Pleistocene and recent humans, Niewoehner (2000, 2001, 2005) investigated the three-dimensional (3D) complexity of the joint. The method used by the author consisted in placing landmarks by projecting the image of a grid of specially prepared slides onto the joint surface and using photogrammetry to digitize the landmarks. He then analyzed the data using 3D geometric morphometric methods (GMM), using Procrustes superimposition and principal component analysis (PCA) (Niewoehner, 2005). The analysis revealed that Neanderthals possessed a more dorsovolarly flat tmcj than early Upper Paleolithic, late Upper Paleolithic and modern humans, and did not have the palmar beak present in modern humans. These results were interpreted as evidence of greater power required by Neanderthal manipulatory repertoire compared with late Pleistocene early human manipulatory repertoire (Niewoehner, 2000, 2005; Trinkaus, 1983; Trinkaus and Villemeur, 1991).

In an effort to provide a wider comparative framework, Marzke et al. (2010) analyzed the joint morphology of the mutual trapezial and MC 1 joint surfaces in extant great apes and humans, as well as *Papio*, australopiths, early *Homo* and Neanderthals. The authors quantified and compared curvatures of the joint surfaces by using two 3D approaches: stereophotogrammetry with B-spline surface analysis and laser scanning with quadric surface analysis (Marzke et al., 2010). The results reflect our knowledge on the functional anatomy of tmcj in modern humans and fossil hominins. In particular, they found that human tmcj surfaces (of both MC 1 and the trapezium) are less curved than in great apes, both in radioulnar and dorsovolar directions. In agreement with Niewoehner (2001), they also found that Neanderthals have lower dorsovolar curvature than modern humans in their MC 1 proximal articular surface, suggesting the ability to distribute greater axial joint load. Finally, australopiths' tmcj curvatures are more similar to those of great apes.

The studies of Tocheri et al. (2003, 2005), Niewoehner (2000, 2001, 2005) and Marzke et al. (2010) succeeded in quantifying the complex anatomy of the tmcj surfaces. However, though they are accurate and reflect our knowledge on the functional anatomy of tmcj, they involve complex steps in the estimate of joint surface curvature (Marzke et al., 2010). Moreover, because of the fragmentary nature of some of the comparative fossil material included in his study, Niewoehner (2005) could not map the complete articular surfaces involved in the tmcj, and did not provide data for nonhuman hominids, while the method used by Marzke et al. (2010) quantifies the curvatures of the articular surfaces of the tmcj but does not give any information on other aspects of the joint surfaces.

Due to the increased availability of laser and CT-scanned databases, available also on line (see, for example, www.morphosource.org), 3D virtual reconstructions of bones to study functional morphology has become more accessible in the last decade. Even though GMM utility for addressing questions of phylogeny, systematics, and morphological variation is widely accepted, a growing body of work has shown that it may also be a valuable tool for the assessment of shape variation of postcranial skeletal elements in functional analyses (Brzobohatá et al., 2014; Frelat et al., 2012; Harmon, 2007; Knigge et al., 2015; Turley et al., 2011). Placing landmarks on 3D models of CT- or laser-scanned bones is less complicated than using the photogrammetry methods used in previous studies.

In this paper, we aim to quantify the overall morphology of one of the two articular surfaces of the tmcj, in particular the proximal articular surface of MC 1, using a 3D GMM approach on a sample of CT- and laser-scanned MC 1s including extant human and nonhuman hominids, and South African hominin fossils, in an attempt at pooling the strengths of the studies performed previously and expanding their results (Marzke et al., 2010; Niewoehner, 2000, 2001, 2005). More specifically, the present study quantifies the proximal articular surface of MC 1 using the 3D GMM approach in extant hominids (*Homo*, *Pan*, *Gorilla* and *Pongo*) and two fossil hominin MC 1s from South Africa (SK 84, *Paranthropus robustus*/*Homo erectus* and StW 418, *Australopithecus africanus*) to test the following hypotheses: (1) the MC 1 proximal articular surface of humans will be less curved in both radioulnar and dorsovolar aspects than nonhuman hominids, as representing skeletal correlates to greater loads of the human MC 1 proximal articular surface necessary for forceful precision grip and greater mobility of the joint than in nonhuman hominids (Marzke et al., 2010; Rose, 1992); (2) the MC 1 proximal articular surface of nonhuman hominids will be similar in different species. Nonhuman hominids use their thumb similarly for manipulative tasks (Napier, 1960) and rarely for locomotor purposes, mainly for power grip during climbing (Lewis, 1977; Napier, 1960; Tuttle, 1969). The only exception may be in *Gorilla*, where greater dorsovolar curvature due to association with their forceful pulling and processing of vegetation has been described (Marzke, 2006; Marzke et al., 2010); (3) the MC 1 proximal articular surface of SK 84 will most closely resemble that of *Homo* in our sample (Marzke et al., 2010; Skinner et al., 2015; Tocheri et al., 2008). SK 84 has been in the past classified as *H. erectus* (Susman, 1988, 1994) or *P. robustus* (Trinkaus and Long, 1990). Though previous studies suggested that SK 84 morphology and therefore function was closer to chimpanzees than to modern humans (Lewis, 1977; Rightmire, 1972), more recent anatomical investigations proposed it to belong to the hand of a hominin capable of stone tool-making (Tocheri et al., 2008); and (4) the MC 1 proximal articular surface of StW 418 will most closely resemble that of the nonhuman hominids in our sample (Green and Gordon, 2008; Susman, 1994; Tocheri et al., 2008). The morphology of *A. africanus* suggests that they did not have the full suite of traits associated with adaptations to forceful precision gripping (Green and Gordon, 2008; Susman, 1994; Tocheri et al., 2008; but see Skinner et al., 2015), which characterize modern humans, and therefore may have used their hands for arboreal locomotion (McHenry and Berger, 1998) and be more similar to nonhuman hominids than to humans.

2. Materials and methods

The MC 1 proximal articular surface was examined in a sample made up by *H. sapiens* ($n = 18$, 8 males and 10 females), *Pan troglodytes* ($n = 14$, 8 males and 6 females), *Gorilla gorilla* ($n = 14$, 9 males and 5 females), *Pongo pygmaeus* ($n = 8$, 4 males and 4 females), *Pongo abelii* ($n = 1$, female), and fossil hominins (SK 84, cf. *P. robustus/H. erectus* and StW 418, *A. africanus*). Only two fossil specimens were available for this study. Many proximal MC 1 are however available in the fossil record, for example *A. afarensis* (Green and Gordon, 2008; Rolian and Gordon, 2013), *A. sediba* (Kivell et al., 2011) and *H. naledi* (Kivell et al., 2015), to which this method could be applied to evaluate the manipulatory capabilities of these species.

Nonhuman hominid specimens were collected at the Anthropologische Staatssammlung at the University of Munich, Germany. The human specimens were collected at the Raymond A. Dart Collection, University of the Witwatersrand, South Africa. The fossil specimens were collected at the Evolutionary Studies Institute and Centre of Excellence in Palaeosciences, University of the Witwatersrand, South Africa. Only adult individuals, as evinced from fully fused epiphyses, were included in the study. Individuals with signs of pathological alterations in the postcranial skeleton were excluded from this study to avoid biases due to possible different mechanical loadings in their limbs.

Medical CT scanning of the first metacarpals of chimpanzees, gorillas, orangutans and modern humans were performed at the University of Munich Institute for Radiology, Germany, on a GE CT750 HD Discovery medical CT scanner (pixel dimensions 0.46×0.46 mm) and at the University Hospital of Zurich, Switzerland, on a Siemens Somatom Definition Flash (pixel dimensions 0.60×0.60 mm). The fossil specimen StW 418 was micro CT-scanned at the University of the Witwatersrand Microfocus X-ray Computed Tomography Facility, on a Nikon Metrology XTH 225/320 LC dual source industrial CT system (pixel dimensions 0.0137×0.0137 mm). Following data acquisition, image stacks were segmented to produce isosurfaces using Avizo 8.1 software (Visualization Sciences Group, Mérignac, France). The fossil specimen SK 84 was laser-scanned (Next Engine laser scanner) at the Ditsong Museum, Pretoria, South Africa.

Articular surfaces were analyzed using landmarks placed with the software Landmark Editor (Wiley et al., 2005). Landmarks were chosen to capture the overall shape and curvature of the surface (see Fig. 1 and Table 1). Landmarks were subjected to a Generalized Procrustes Analysis (GPA) using sliding landmarks and principle components analysis (PCA) in R with the Geomorph package (Adams and Otarola-Castillo, 2013; Adams et al., 2015; Gower, 1975; O'Higgins and Jones, 1998). We used a series of sliding semi-landmark curves to capture the shape of the articular surface, with the most volar and dorsal points along each as anchor. For example, the point C1 and its dorsal counterpart are the anchors along the C1 curve, with the landmarks in between being slid (see Fig. 1).

Morphologika was used to visualize shape as wireframes in relation to principle component scores (Fig. 2). Significant differences among principle component (PC) scores were tested using an analysis of variance (ANOVA) and Tukey HSD post-hoc test was used to identify the extant groups that are significantly different. Boxplots were used to graphically represent data distributions. Fossils

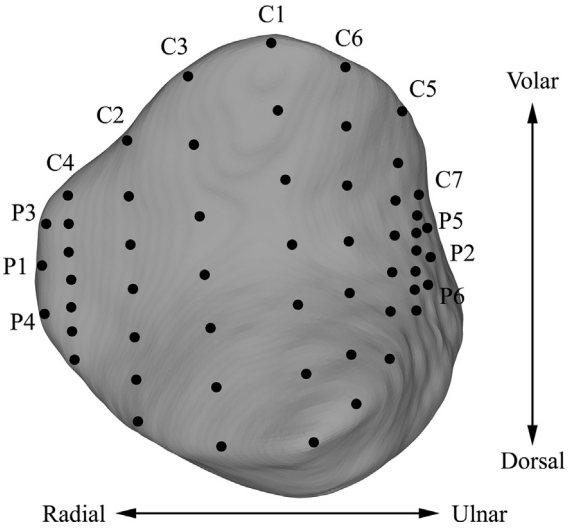

Fig. 1. Landmarks on the metacarpal 1 proximal articular surface.
Fig. 1. Points repères sur la surface articulaire proximale du métacarpe 1.

Table 1
Landmark explanations.
Tableau 1
Définition des points repères.

Landmark	Description
C1	The volar point is the most proximal point on the boundary of the articular surface in the volar aspect. The dorsal point is the most proximal point on the boundary of the articular surface in the dorsal direction
C2	The volar point is the midpoint between P1and the volar point of C1. The dorsal point is the midpoint between P1and the dorsal point of C1
C3	The volar point is the midpoint between the volar point of C1 and the volar point of C2. The dorsal point is the midpoint between the dorsal point of C1 and the dorsal point of C2
C4	The volar point is the midpoint between P1 and the volar point of C2. The dorsal point is the midpoint between P1 and the dorsal point of C2
C5	The volar point is the midpoint between P2 and the volar point of C1. The dorsal point is the midpoint between P2 and the dorsal point of C1
C6	The volar point is the midpoint between the volar point of C1 and the volar point of C5. The dorsal point is the midpoint between the dorsal point of C1 and the dorsal point of C5
C7	The volar point is the midpoint between P2 and the volar point of C5. The dorsal point is the midpoint between P2 and the dorsal point of C5
P1	The most radial point on the boundary of the articular surface in the radial aspect
P2	The most ulnar point on the boundary of the articular surface in the ulnar aspect
P3	The midpoint between P1 and the volar point of C4
P4	The midpoint between P1 and the dorsal point of C4
P5	The midpoint between P2 and the volar point of C7
P6	The midpoint between P2 and the dorsal point of C7

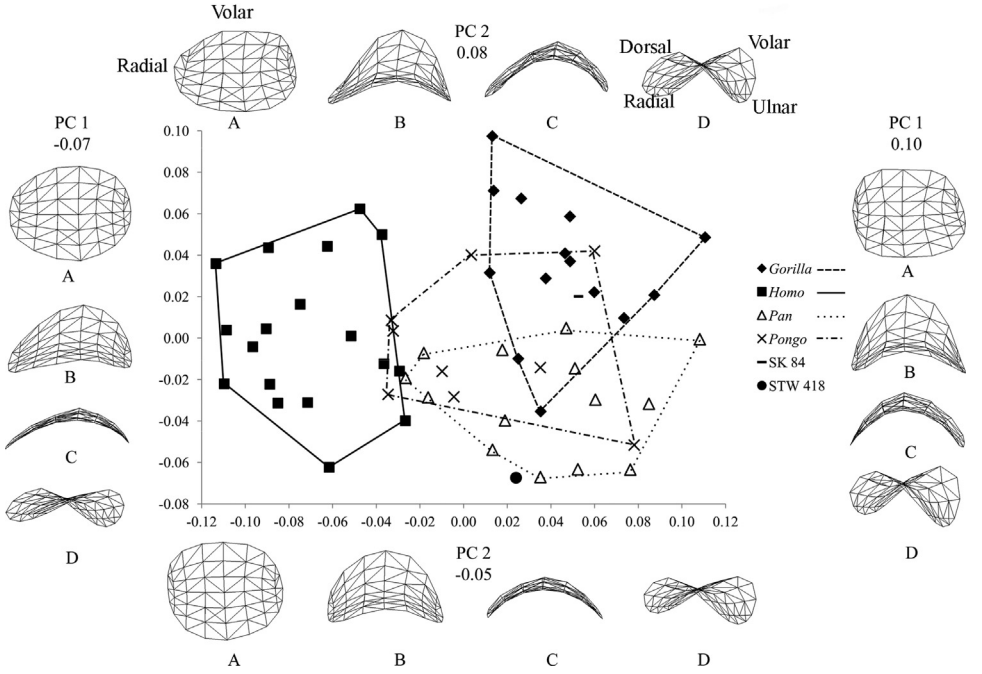

Fig. 2. Plots of Principal Component (PC) 1 and PC 2 scores of extant samples (*Homo*, *Pan*, *Gorilla* and *Pongo*) and fossil specimens (SK 84, *Paranthropus robustus/Homo erectus* and StW 418, *Australopithecus africanus*). The wireframes show extreme shape for each axis, with shape representing the PC value indicated. For each wireframe, radial is on the left and volar is superiorly. The wireframes labeled (A) are MC 1 proximal articular surface in proximal view; the wireframes labeled (B) are the MC 1 proximal articular surface tilted with the volar aspect to the foreground; the wireframes labeled (C) are the MC 1 proximal articular surface pointed upward oriented to view radioulnar curvature; the wireframes labeled (D) are the MC 1 proximal articular surface in dorsal view tilted ulnarly to show the curvature in the dorsovolar aspect.

Fig. 2. Graphiques de l'analyse en composantes principales (PC) montrant les résultats de PC1 et PC2 pour les échantillons actuels (*Homo*, *Pan*, *Gorilla* et *Pongo*) et les spécimens fossiles (SK 84, *Paranthropus robustus/Homo erectus* et StW 418, *Australopithecus africanus*). Les représentations en fil de fer illustrent les conformations extrêmes pour chaque axe, avec la conformation représentant la valeur indiquée pour PC. Pour chaque représentation en fil de fer, l'aspect radial est à gauche et l'aspect palmaire est en haut. Les représentations en fil de fer nommées (A) correspondent à la surface articulaire proximale du MC1 en vue proximale ; celles nommées (B) représentent la surface articulaire proximale du MC1 inclinée, avec l'aspect palmaire en arrière-plan ; celles nommées (C) montrent la surface articulaire proximale du MC1 orientée vers le haut, afin de voir la courbure radio-ulnaire ; celles nommées (D) illustrent la surface articulaire proximale du MC1 en vue dorsale inclinée en direction ulnaire pour montrer la courbure de l'aspect dorso-palmaire.

were evaluated relative to the comparative extant samples through visual comparison with group distributions in the boxplots and by using comparative group means and standard deviations with the distance between the fossil specimen and each extant group expressed as the number of SDs from that group's mean. Differences were considered significant when the fossil specimens were more than 1 SD away from the mean of extant groups (Marchi et al., 2016).

3. Results

In the principal component analysis, PC 1 explains 31.4% of the variation between specimens, and PC 2 explains 13.4% of the variation. Principle components 3 and beyond are not informative in terms of shape and are not included in these results. The ANOVA to compare principle components scores between groups yielded a significant result for PC 1 ($P < 0.001$) and PC 2 ($P < 0.001$). The Tukey HSD post-hoc test yielded a significant difference in PC 1 (Table 2) between *Homo* and all ape groups ($P < 0.00$ for all comparisons). For PC 2 (Table 3), the post-hoc test yielded a significant result for several comparisons. *Gorilla* is significantly different from all other groups (*Homo*, $P = 0.02$; *Pan*, $P < 0.00$; *Pongo* $P = 0.02$). *Pan* is also significantly different from *Homo* ($P = 0.04$). *Homo* is significantly different from *Pan* and *Gorilla*, but not *Pongo*.

Wireframes are used to show shape as reflected on each PC axes (Fig. 2). Shape is shown from the following four perspectives on each axis: proximal, proximal angled to the foreground, dorsal, dorsal with ulnar view.

3.1. PC 1 shape and groupings

The shape represented on the PC 1 axis is most informative in distinguishing *Homo* from the ape groups. The negative side of the PC 1 axis is occupied primarily by *Homo*, and shows a relatively flat articular surface in the radioulnar and dorsovolar aspects. In addition, the surface is extended and slightly narrowed in the radial aspect. The positive side of the PC 1 axis is occupied by the ape groups. The joint surface on this portion of the axis lacks radial extension and is highly curved in both dorsovolar and radioulnar aspects. The greater dorsovolar curvature observable in the dorsal view tilted ulnarly (Fig. 2) creates a longer and more proximally projecting volar beak in apes. The fossil specimens SK 84 and StW 418 overlap the ape groups on the PC 1 axis (Fig. 3a, Table 4), with SK 84 within

Table 2
Principal Component 1 scores, Tukey HSD post-hoc test multiple comparisons among *Homo*, *Pan*, *Gorilla* and *Pongo*.
Tableau 2
Valeurs de la composante principale 1, test post-hoc Tukey HSD de comparaisons multiples entre *Homo*, *Pan*, *Gorilla* et *Pongo*.

Group	Mean difference	SE	*P*	95% Confidence Interval	
				Lower Bound	Upper Bound
Homo					
Gorilla	−0.12	0.01	0.00*	−0.15	−0.09
Pan	−0.11	0.01	0.00*	−0.14	−0.07
Pongo	−0.08	0.01	0.00*	−0.12	−0.04
Pan					
Gorilla	−0.01	0.01	0.84	−0.05	0.02
Homo	0.11	0.01	0.00*	0.07	0.14
Pongo	0.03	0.01	0.28	−0.01	0.07
Gorilla					
Homo	0.12	0.01	0.00*	0.09	0.15
Pan	0.01	0.01	0.84	−0.02	0.05
Pongo	0.04	0.01	0.06**	0.00	0.08
Pongo					
Gorilla	−0.04	0.01	0.06**	−0.08	0.00
Homo	0.08	0.01	0.00*	0.04	0.12
Pan	−0.03	0.01	0.28	−0.07	0.01

* $P < 0.05$.
** $0.05 < P < 0.010$.

Table 3
Principal Component 2 scores, Tukey HSD post-hoc test multiple comparisons among *Homo*, *Pan*, *Gorilla* and *Pongo*.
Tableau 3
Valeurs de la composante principale 2, test post-hoc Tukey HSD de comparaisons multiples entre *Homo*, *Pan*, *Gorilla* et *Pongo*.

Group	Mean difference	SE	*P*	95% Confidence Interval	
				Lower Bound	Upper Bound
Homo					
Gorilla	−0.03	0.01	0.02*	−0.06	0.00
Pan	0.03	0.01	0.04*	0.00	0.06
Pongo	0.01	0.01	0.95	−0.03	0.04
Pan					
Gorilla	−0.07	0.01	0.00*	−0.10	−0.03
Homo	−0.03	0.01	0.04*	−0.06	0.00
Pongo	−0.02	0.01	0.28	−0.06	0.01
Gorilla					
Homo	0.03	0.01	0.02*	0.00	0.06
Pan	0.07	0.01	0.00*	0.03	0.10
Pongo	0.04	0.01	0.02*	0.00	0.08
Pongo					
Gorilla	−0.04	0.01	0.02*	−0.08	0.00
Homo	−0.01	0.01	0.95	−0.04	0.03
Pan	0.02	0.01	0.28	−0.01	0.06

* $P < 0.05$.

Table 4
Mean Principal Component (PC) 1 and PC 2 scores for *Homo*, *Pan*, *Gorilla* and *Pongo* compared with PC scores of fossil specimens SK 84 (*Paranthropus robustus/Homo erectus*) and StW 418 (*Australopithecus africanus*).
Tableau 4
Valeurs moyennes des composantes principales (PC) 1 et PC2 pour *Homo*, *Pan*, *Gorilla* et *Pongo*, comparées avec les valeurs PC des spécimens fossiles SK 84 (*Paranthropus robustus/Homo erectus*) et StW 418 (*Australopithecus africanus*).

Group	*Homo* Mean (SD) ($n = 18$)	*Pan* Mean (SD) ($n = 14$)	*Gorilla* Mean (SD) ($n = 14$)	*Pongo* Mean (SD) ($n = 9$)	SK 84	StW 418
PC 1	−0.071 (0.028)	0.036 (0.040)	0.046 (0.029)	0.007 (0.042)	$0.053^{a}{}_{H,Po}$	0.024_{H}
PC 2	0.001 (0.035)	−0.030 (0.025)	0.035 (0.034)	−0.005 (0.031)	0.020_{P}	$-0.067_{H,P,G,Po}$

[a] The fossil specimen indicates at least 1 SD from the mean of: *Homo* = H; *Pan* = P; *Gorilla* = G; *Pongo* = Po.

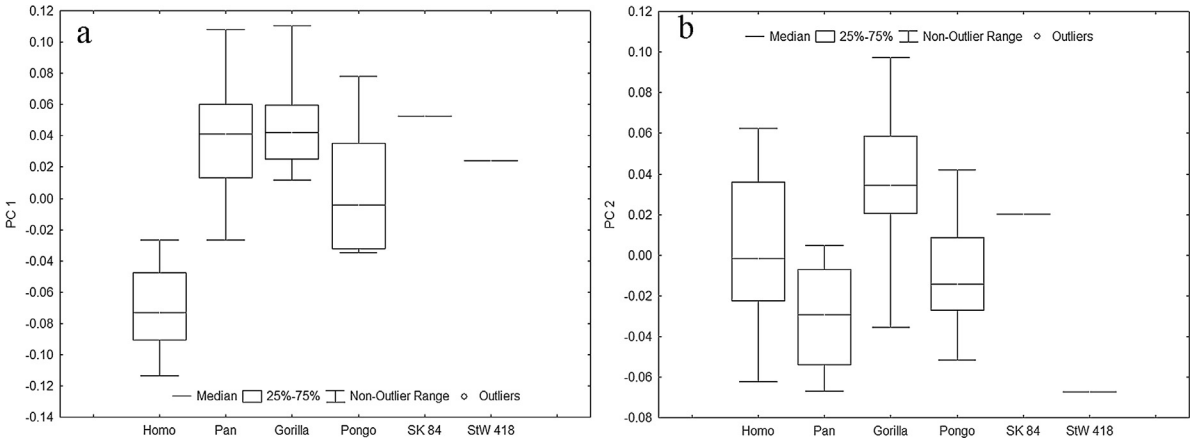

Fig. 3. Boxplot of Principal Component (PC) scores for *Homo*, *Pan*, *Gorilla* and *Pongo* compared with fossil specimens, SK 84 (*Paranthropus robustus/Homo erectus*) and StW 418 (*Australopithecus africanus*). (a) PC 1; (b) PC 2.
Fig. 3. Graphique des valeurs de l'analyse en composantes principales (PC) pour *Homo*, *Pan*, *Gorilla* et *Pongo*, comparées à celles des spécimens fossiles, SK 84 (*Paranthropus robustus/Homo erectus*) et StW 418 (*Australopithecus africanus*). (a) PC 1 ; (b) PC 2.

the interquartile range of African apes and StW 418 within the interquartile range of *Pan* and *Pongo*.

3.2. PC 2 shape and groupings

Shape on the PC 2 axis is most informative in distinguishing between ape groups. The positive portion of the PC 2 axis, occupied mostly by *Gorilla*, represents slightly greater curvature in the dorsovolar and radioulnar aspects relative to the negative portion of this axis. In addition, there is radial extension associated with this curvature, slight concavity in the radial area and slightly longer volar beak, predominantly in *Gorilla*. The negative aspect of the PC 2 axis, occupied mostly by *Pan*, is slightly less curved in the radioulnar and dorsovolar aspects, and the radial portion of the surface is reduced with some flattening of the ulnar aspect. *Pongo* occupies an intermediate location on this axis, which overlaps both *Gorilla* and *Pan*. The boxplot of PC 2 scores shows that the fossil SK 84 is within the interquartile range of *Homo* and *Gorilla*, but most closely grouped with *Gorilla* (Fig. 3b, Table 4), and StW 418 is lower than all extant species and in the lower quartile range of *Pan*.

4. Discussion

The overall goal of this paper was to quantify the 3D morphology of the MC 1 proximal articular surface using 3D GMM on virtually reconstructed MC 1 bones. We tested four distinct hypotheses: (1) the MC 1 proximal articular surface of humans will be less curved in both radioulnar and dorsovolar aspects than nonhuman hominids; (2) the MC 1 proximal articular surface of nonhuman hominids will be similar in the different species analyzed here; (3) the MC 1 proximal articular surface of SK 84 will most closely resemble *Homo*; (4) the MC 1 proximal articular surface of StW 418 will most closely resemble the nonhuman hominids. The results obtained are in general agreement with previous results (Marzke et al., 2010; Niewoehner, 2000, 2001, 2005; Tocheri et al., 2003, 2005), proving the validity of the method in testing the morphology of the MC 1 proximal articular surface.

Results show that *Homo* is significantly different from all nonhuman hominids. Hypothesis 1 cannot therefore be falsified. The shape on the PC 1 axis represents a highly curved joint surface in the radioulnar and dorsovolar aspects in nonhuman hominids, a relatively flatter surface in both aspects for *Homo*, and the presence of a volar beak on the volar aspect of nonhuman hominids as observed previously by Marzke et al. (2010). However, the analysis of the 3D shape of the joint surface performed here highlights other characteristics that were not possible to point out using joint curvatures (Marzke et al., 2010). *Homo* is characterized by a radially extended surface that is not present in nonhuman hominids. In a previous study, Rose (1992) found that the greater abduction-adduction range in the living hominoids compared to nonhominoid primates is reflected in MC 1 in a greater radial extension of the MC 1 proximal articular surface. In many human manipulative activities, like precision grip, the thumb is highly abducted, therefore the load is radially shifted on the joint surface (Lewis, 1977; Marzke et al., 2010; Rose, 1992). To have the necessary stability in a joint, the joint itself needs to resist displacement in a given direction (Hamrick, 1996), in this case in the radial direction. The radial extension observed in the 3D GMM analysis of the human MC 1 proximal articular surface therefore provides a larger contact area for the abducted MC 1 in grasp contributing to the stability of the human tmcj.

The nonhuman hominid groups are not significantly different from one another on PC1. On PC2, though overlap is present between *Pongo* and *Pan*, *Gorilla* is moderately separated from the other groups. Hypothesis 2 is therefore only partially falsified. Nonhuman hominids use their lateral fingers mainly in hook-like grips when moving in trees, keeping the thumb out of the way during such activities. When on the ground, African great apes knuckle-walk, a type of locomotion that does not involve the thumb (Tuttle, 1967). *Pongo*, when on the ground, place their hands in any number of varied postures with the dorsum of the proximal

phalanges of the lateral fingers apposed to the substrate, or use palmigrady. In general, the thumb is not used for weight support (Susman, 1994; Tuttle, 1967). When climbing up trees, on the other hand, all nonhuman hominids use their thumb in power grip-like fashion to firmly grasp the support they are climbing on (Lewis, 1977; Tuttle, 1969). On the basis of the similar use nonhuman hominids make of the thumb, we would expect similar loads on their MC 1 proximal articular surface, and therefore similar shape of the joint surface, as previous studies have found (Marzke et al., 2010). However, by analyzing MC 1 proximal articular surface curvature, Marzke and colleagues observed an exceptionally high dorsovolar curvature on the MC 1 proximal articular surface. Our analysis partially separates *Gorilla* from all other hominids on PC2. The positive portion of PC2, where *Gorilla* fell, is characterized by greater curvature in the dorsovolar and radioulnar aspects relative to the negative portion of this axis. Marzke et al. (2010) suggested that the greater dorsovolar curvature of *Gorilla* could favor tmcj stability and could be a consequence of the observed forceful pulling and processing of vegetation by gorillas (Marzke, 2006). Our results further point to the greater stability in the *Gorilla* tmcj compared to the other nonhuman hominid joint, providing also evidence of greater radioulnar curvature. In order to test this hypothesis, more studies are necessary to properly describe the observed forceful pulling behavior by *Gorilla*.

The 3D shape analysis of the MC 1 proximal articular surface also displays a radial extension of the *Gorilla* joint surface associated with slight concavity in the radial area. Though all great apes use their hand in complex manipulatory tasks (Byrne et al., 2001; Christel, 1993), *Gorilla* shows the thumb-to-finger proportions most similar to *Homo* among nonhuman hominids (Tuttle, 1969). Because of the similarity in length proportions, it is possible that *Gorilla* needs greater abduction of MC 1 when grasping trees during climbing, and this greater abduction may require radially extended MC 1 proximal articular surface compared to the other nonhuman hominids (Rose, 1992). Kinetic studies of the hand of climbing *Gorilla* (and other nonhuman hominids) are necessary to further explore this hypothesis.

Both fossil specimens most closely resemble the nonhuman hominids, and do not overlap *Homo* on the PC 1 axis. Hypothesis 3 is therefore falsified, while hypothesis 4 cannot be falsified. The specimen StW 418 occupies a location for PC 1 and PC 2 that shows a relatively shallower surface in the radioulnar and the dorsovolar aspects, shows the typical volar beak of apes, and lacks the radial extension of the surface associated with *Homo*. SK 84 occupies a similar location to StW 418 on PC 1, but it is on the opposite side of the axis for PC 2. Its location shows a surface that is longer and more highly curved in the radioulnar aspect compared to StW 418. SK 84, similar to StW 418, also shows the typical volar beak of apes and lacks the radial extension associated with *Homo*.

Previous studies on StW 418 are rare, but several studies have investigated SK 84. The gracility (Napier, 1959) and strongly curved proximal articular surface of SK 84 (Tocheri, 2007) are both primitive features of the fossil, similar to what our study suggests. However, SK 84 shows the modern human first dorsal interosseous muscle morphology, which provides a longer moment arm for adduction of the thumb than seen in the great apes (Tocheri et al., 2008). Susman (1994), on the basis of linear measurements, proposed that SK 84 exhibited derived pollical morphologies indicating refined precision grips. These interpretations are in contrast to the ones obtained by the study of the 3D GMM of the MC 1 proximal articular surface, which suggests a general ape-like morphology for SK84.

A recent study on the trabecular structure of MCs (Skinner et al., 2015) found for SK 84 and StW 418 a mosaic trabecular pattern between that of *Homo* and nonhuman hominids, as we would expect. The two fossils exhibit high trabecular bone volume fraction similar to *Pan* and different from the lower trabecular density of recent *Homo*. However, the authors found that the distribution of trabecular bone is similar to the patterns of committed tool users such as *H. sapiens* and *H. neanderthalensis*. Skinner et al. (2015) conclude suggesting that the South African hominins show evidence of forceful and habitual human-like opposition of the thumb and fingers that is necessary for power and precision grips, providing evidence of committed tool use in those hominins.

While we agree that trabecular bone anatomy provides evidence of the actual load to which a bone is subjected in life (Kivell, 2016), we also think that external bone morphology – and joint in particular though more genetically and functionally constrained (Currey, 2002; Ruff, 1988; Ruff and Runestad, 1992; Ruff et al., 1994) – can tell us much about early hominin behavior. The trabecular information provided by Skinner and colleagues may very well tell as that South African hominins were loading their MC 1 proximal articular surface in a way similar to modern humans – in agreement with Tocheri et al. (2008) observation on the insertion of first dorsal interosseous muscle on SK 87 – but the articular shape informs us on the type and range of movements that were possible at the level of the articulation (but see Chan, 2008). The MC 1 proximal articular surface of SK 84 and StW 418 were more ape-like than *Homo*-like in their morphology and, according to the many studies performed on the anatomy and function of this articulation (Lewis, 1977; Marzke et al., 2010; Napier, 1955, 1956, 1960; Niewoehner, 2000, 2001, 2005; Rose, 1992; Susman, 1994, 1988; Tocheri, 2007; Tocheri et al., 2008; Tuttle, 1967, 1969), we suggest that the hands to which the two fossils belonged may not have been able to perform the full range of abduction-adduction movements that we associate today with stone tool-making and use (Marzke, 1997, 2006). This does not mean that *A. africanus* and *P. robustus* (or *H. erectus*, depending on what SK 84 is considered to be) and other early hominins were not able to produce and use stone tools, but that if they were making stone tools (like not only the trabecular studies – Skinner et al., 2015 – but also archeological studies – Harmand et al., 2015 – seem to suggest) they were making them in a different way as later *Homo* and modern humans are doing. This could imply that the behavior of making and using stone tools preceded the morphological adaptations that we associate today to such behavior. More fossil hand bones and more studies, for example looking at the MC 1 facet on associated trapezia to investigate joint

congruence between the two bones, are necessary to test this hypothesis, but the current evidence seems to point in that direction.

5. Conclusions

The aim of this paper was to provide a method to interpret the overall shape of the MC 1 proximal articular surface in relation to manipulatory abilities in living apes and humans. Overall the three-dimensional characterization of the proximal MC 1 articular surface is in agreement with previous studies that used different methods to quantify articular curvature. In particular:

- the MC 1 proximal articular surface of *Homo* is less curved than that of nonhuman hominids in both the radioulnar and the dorsovolar aspect. Moreover, *Homo* shows radial elongation of the joint suggesting greater abduction during precision grip;
- the MC 1 proximal articular surface of nonhuman hominids is more curved in both radioulnar and dorsovolar aspects than in *Homo* and is generally similar within nonhuman hominids. The only exception is the greater radioulnar and dorsovolar curvature of *Gorilla* than *Pan* and *Pongo*, associated with a greater volar beak which may be due to the forceful pulling of vegetation observed for the genus;
- the MC 1 proximal articular surface of SK 84 and StW 418 shows an ape-like MC 1 proximal articular surface shape. Considering the presence of stone tools associated with early hominins and the trabecular structure of MC 1 proximal joint, this may indicate that South African hominins may have been able to produce and use stone tools but lacked the distinctive human morphology that facilitates forceful precision and power grips.

Acknowledgements

We wish to thank Roberto Macchiarelli and Clément Zanolli for inviting us to contribute to the thematic issue in memory of Laurent Puymerail. D.M. recalls he got in contact with Laurent to discuss about a collaboration on the morphometric maps of the femur of fossil hominins; in his unfortunately too brief career Laurent gave an important contribution to the application of the morphometric map method to study long bone biomechanics and this special issue is the right acknowledgement of his work. We also wish to thank Karin Isler, University of Zurich, Irchel, Switzerland and Gisela Grupe, University of Munich, Germany for access to specimens in their care. The University of Munich Institute for Radiology in the person of Jochen Grimm for kindly assisting when taking medical CT-scans of the Munich material. Brendon Billings for access to the human specimens in the Raymond A. Dart Collection and Bernard Zipfel for access to the CT-scans of the fossils in the Evolutionary Studies Institute and Centre of Excellence in Palaeosciences at the University of the Witwatersrand, South Africa. Tracy Kivell and Matt Tocheri for precious comments on an earlier version of the manuscript.

References

Adams, D.C., Otarola-Castillo, E., 2013. Geomorph: an R package for the collection and analysis of geometric morphometric shape data. Meth. Ecol. Evol. 4, 393–399.
Adams, D.C., Collyer, M.L., Sherratt, E., 2015. Geomorph: Software for Geometric Orphometric Analyses. R Package Version 2.1.x. http://cran.r-oject.org/web/packages/geomorph/index.html.
Aiello, L., Dean, M.C., 1990. An Introduction to Human Evolutionary Anatomy. Elsevier Academic Press, London (596 p.).
Almécija, S., Moyà-Solà, S., Alba, D.M., 2010. Early origin for human-like precision grasping: a comparative study of pollical distal phalanges in fossil hominins. PloS ONE 5, e11727.
Almécija, S., Smaers, J.B., Jungers, W.L., 2015. The evolution of human and ape hand proportions. Nat. Comm. 6, 7717, http://dx.doi.org/10.1038/ncomms8717.
Berger, L.R., de Ruiter, D.J., Churchill, S.E., Schmid, P., Carlson, K.J., Dirks, P.H.G.M., Kibii, J.B., 2010. *Australopithecus sediba*: a new species of *Homo*-like australopith from South Africa. Science 328, 195–204.
Berger, L.E., Hawks, J., de Ruiter, D.J., Churchill, S.E., Schmid, P., Delezene, L., Kivell, T., Garvin, H.M., Williams, S.A., DeSilva, J.M., Skinner, M.M., Musiba, C.M., Cameron, N., Holliday, T.W., Harcourt-Smith, W., Ackermann, R.R., Bastir, M., Bogin, B., Bolter, D., Brophy, J., Cofran, Z.D., Congdon, K.A., Deane, A.S., Dembo, M., Drapeau, M., Elliott, M., Feuerriegel, E.M., Garcia-Martinez, D., Green, D.J., Gurtov, A., Irish, J.D., Kruger, A., Laird, M.F., Marchi, D., Meyer, M.R., Nalla, S., Negash, E.W., Orr, C.M., Radovcic, D., Schroeder, L., Scott, J.E., Throckmorton, Z., Tocheri, M.W., VanSickle, C., Walker, C.S., Wei, P., Zipfel, B., 2015. A new species of the genus *Homo* from the Dinaledi Chamber, South Africa. eLIFE 4, e09560.
Brzobohatá, H., Krajíček, V., Velemínský, P., Poláček, L., Velemínská, J., 2014. The shape variability of human tibial epiphyses in an early medieval Great Moravian population (9th–10th century AD): a geometric morphometric assessment. Anthropol. Anzeig. 71, 219–236.
Byrne, R.W., Corp, N., Byrne, J.M.E., 2001. Manual dexterity in the gorillas: bimanual and digit role differentiation in a natural task. Anim. Cogn. 4, 347–361.
Chan, L.K., 2008. The range of passive arm circumduction in primates: do hominoids really have more mobile shoulders? Am. J. Phys. Anthropol. 136, 265–277.
Christel, M., 1993. Grasping techniques and hand preferences in Hominoidea. In: Preuschoft, H., Chivers, D.J. (Eds.), Hands of Primates. Springer Verlag, Wien, pp. 91–108.
Coffing, K.E., (Ph.D. dissertation) 1998. The metatarsals of *Australopithecus afarensis*: Locomotor and Behavioral Implications of Cross-Sectional Geometry. Johns Hopkins University, Baltimore.
Currey, J.D., 2002. Bones: Structure and Mechanics. Princeton University Press, Princeton (436 p.).
Frelat, M., Stanislav, K., Weber, G., Bookstein, F., 2012. Technical note: a novel geometric morphometric approach to the study of long bone shape variation. Am. J. Phys. Anthropol. 149, 628–638.
Gower, J.C., 1975. Generalized Procrustes analysis. Psychom. 40, 33–51.
Green, D.J., Gordon, A.D., 2008. Metacarpal proportions in *Australopithecus africanus*. J. Hum. Evol. 54, 705–719.
Hamrick, M.W., 1996. Functional morphology of the lemuriform wrist joints and the relationship betweeen wrist morphology and positional behavior in arboreal primates. Am. J. Phys. Anthropol. 99, 319–344.
Hamrick, M.W., Churchill, S.E., Schmitt, D., Hylander, W.L., 1998. EMG of the human flexor pollicis longus muscle: implications for the evolution of hominid tool use. J. Hum. Evol. 34, 123–136.
Harmand, S., Lewis, J.E., Feibel, C.S., Lepre, C.J., Prat, S., Lenoble, A., Boës, X., Quinn, R.L., Brenet, M., Arroyo, A., Taylor, N., Clément, S., Daver, G., Brugal, J.-P., Leakey, L., Mortlock, R.A., Wright, J.D., Lokorodi, S., Kirwa, C., Kent, D.V., Roche, H., 2015. 3.3-million-year-old stone tools from Lomekwi 3, West Turkana, Kenya. Nature 521, 310–315.
Harmon, E.H., 2007. The shape of the hominoid proximal femur: a geometric morphometric analysis. J. Anat. 210, 170–185.
Kivell, T.L., 2015. Evidence in hand: recent discoveries and the early evolution of human manual manipulation. Phil. Trans. R. Soc. B 370, 20150105.
Kivell, T.L., 2016. A review of trabecular bone functional adaptation: what have we learned from trabecular analyses in extant hominoids and what can we apply to fossils? J. Anat. 228, 569–594.
Kivell, T.L., Deane, A.S., Tocheri, M.W., Orr, C.M., Schmid, P., Hawks, J., Berger, L.R., Churchill, S.E., 2015. The hand of *Homo naledi*. Nat. Comm. 6, 8431.
Kivell, T.L., Kibii, J.M., Churchill, S.E., Schmid, P., Berger, L.R., 2011. *Australopithecus sediba* hand demonstrates mosaic evolution of locomotor and manipulative abilities. Science 333, 1411–1417.

Knigge, R.P., Tocheri, M.W., Orr, C.M., McNulty, K.P., 2015. Three-dimensional geometric morphometric analysis of talar morphology in extant gorilla taxa from highland and lowland habitats. Anat. Rec. 298, 277–290.
Lewis, O.J., 1977. Joint remodelling and the evolution of the human hand. J. Anat. 123, 157–201.
Marchi, D., Ruff, C.B., Capobianco, A., Rafferty, K.L., Habib, M.B., Patel, B.A., 2016. The locomotion of *Babakotia radofilai* inferred from epiphyseal and diaphyseal morphology of the humerus and femur. J. Morph., http://dx.doi.org/10.1002/jmor.20569.
Marzke, M.W., 1997. Precision grips, hand morphology, and tools. Am. J. Phys. Anthropol. 102, 91–110.
Marzke, M.W., 2006. Who made stone tools? In: Roux, V., Bril, B. (Eds.), Stone Knapping: The Necessary Conditions for a Uniquely Hominin Behaviour. University of Cambridge, Cambridge, McDonald Institute for Archaeological Research, Cambridge, pp. 243–255.
Marzke, M.W., Tocheri, M.W., Steinberg, B., Femiani, J.D., Reece, S.P., Linscheid, R.L., Orr, C.M., Marzke, R.F., 2010. Comparative 3D quantitative analyses of trapeziometacarpal joint surface curvatures among living catarrhines and fossil hominins. Am. J. Phys. Anthropol. 141, 38–51.
McGrew, W.C., 1995. Review of S. Savage-Rumbaugh and R. Lewin's Kanzi: the ape at the brink of the human mind. Hum. Ethol. Bull. 10 (4), 14–16.
McHenry, H.M., 1983. The capitate of *Australopithecus afarensis* and *A. africanus*. Am. J. Phys. Anthropol. 62, 187–198.
McHenry, H.M., Berger, L.R., 1998. Body proportions in *Australopithecus afarensis* and *A. africanus* and the origin of the genus *Homo*. J. Hum. Evol. 35, 1–22.
Napier, J.R., 1955. The form and function of the carpo-metacarpal joint of the thumb. J. Anat. 89, 361–369.
Napier, J.R., 1956. The prehensive movements of the human hand. J. Bone Joint Surg. 38, 902–913.
Napier, J.R., 1959. Fossil metacarpals from Swartkrans. Fossil mammals of Africa No. 17. British Museum of Natural History, London.
Napier, J.R., 1960. Studies of the hand of living primates. Proc. Zool. Soc. London 134, 647–657.
Niewoehner, W.A., (Ph.D. dissertation) 2000. The Functional Anatomy of Late Pleistocene and Recent Human Carpometacarpal and Metacarpophalangeal Articulations. University of New Mexico, New Mexico.
Niewoehner, W.A., 2001. Behavioral inferences from Skhul/Qafzeh early modern human hand remains. Proc. Natl. Acad. Sci. U. S. A. 98, 2979–2984.
Niewoehner, W.A., 2005. A geometric morphometric analysis of Late Pleistocene human metacarpal 1 base shape. In: Slice, D.E. (Ed.), Modern Morphometrics in Physical Anthropology. Kluwer Academic-Plenum Publishers, New York, pp. 285–298.
O'Higgins, P., Jones, N., 1998. Facial growth in *Cercocebus torquatus*: an application of three-dimensional geometric morphometric techniques to the study of morphological variation. J. Anat. 193, 251–272.
Pouydebat, E., Laurin, M., Gorce, P., Bels, V., 2008. Evolution of grasping among anthropoids. J. Evol. Biol. 21, 1732–1743.
Rightmire, G.P., 1972. Multivariate analysis of an early hominid metacarpal from Swartkrans. Science 176, 159–161.
Rolian, C., Gordon, A.D., 2013. Reassessing manual proportions in *Australopithecus afarensis*. Am. J. Phys. Anthropol. 152, 393–406.
Rose, M.E., 1992. Kinematics of the trapezium-1st metacarpal joint in extant anthropoids and Miocene hominoids. J. Hum. Evol. 22, 255–266.
Ruff, C., 1988. Hindlimb articular surface allometry in *Hominoidea* and *Macaca*, with comparisons to diaphyseal scaling. J. Hum. Evol. 17, 687–714.
Ruff, C., Runestad, J.A., 1992. Primate limb bone structure adaptations. Ann. Rev. Anthropol. 21, 407–433.
Ruff, C., Walker, A., Trinkaus, E., 1994. Postcranial robusticity in *Homo*. III: ontogeny. Am. J. Phys. Anthropol. 65, 191–197.
Sarmiento, E.E., 1988. Anatomy of the hominoid wrist joint: its evolutionary and functional implications. Int. J. Primatol. 9, 282–345.
Skinner, M.M., Stephens, N.B., Tsegai, Z.J., Foote, A.C., Nguyen, N.H., Gross, T., Pahr, D.H., Hublin, J.-J., Kivell, T.L., 2015. Human-like hand use in *Australopithecus africanus*. Science 347, 395–399.
Susman, R.L., 1979. Comparative and functional morphology of hominoid fingers. Am. J. Phys. Anthropol. 50, 215–236.
Susman, R.L., 1988. Hand of *Paranthrops robustus* from Member 1, Swartkrans: fossil evidence for tool behavior. Science 240, 781–784.
Susman, R.L., 1991. Species attribution of the Swartkrans thumb metacarpals: reply to Drs. Trinkaus and Long. Am. J. Phys. Anthropol. 86, 549–552.
Susman, R.L., 1994. Fossil evidence for early hominid tool use. Science 265, 1570–1573.
Tocheri, M.W., (Ph.D. dissertation) 2007. Three-Dimensional Riddles of the Radial Wrist: Derived Carpal and Carpometacarpal Joint Morphology in the Genus *Homo* and the Implications for Understanding Stone Tool-Related Behaviors in Hominins. Arizona State University, Arizona.
Tocheri, M.W., Marzke, M.W., Liu, D., Bae, M., Jones, G.P., Williams, R.C., Razdan, A., 2003. Functional capabilities of modern and fossil hominid hands: three-dimensional analysis of trapezia. Am. J. Phys. Anthropol. 122, 101–112.
Tocheri, M.W., Orr, C.M., Jacofsky, M.C., Marzke, M.W., 2008. The evolutionary history of the hominin hand since the last common ancestor of *Pan* and *Homo*. J. Anat. 212, 544–562.
Tocheri, M.W., Razdan, A., Williams, R.C., Marzke, M.W., 2005. 3D quantitative comparison of trapezium and trapezoid relative articular and nonarticular surface areas in modern humans and great apes. J. Hum. Evol. 49, 570–586.
Trinkaus, E., 1983. The Shanidar Neanderthals. Academic Press, New York (502 p.).
Trinkaus, E., 1989. Olduvai hominid 7 trapezial metacarpal 1 articular morphology: contrasts with recent humans. Am. J. Phys. Anthropol. 80, 411–416.
Trinkaus, E., Long, J.C., 1990. Species attribution of the Swartkrans Member 1 first metacarpals: SK 84 and SKX 5020. Am. J. Phys. Anthropol. 83, 419–424.
Trinkaus, E., Villemeur, I., 1991. Mechanical advantages of the Neanderthal thumb in flexion: a test of an hypothesis. Am. J. Phys. Anthropol. 84, 249–260.
Turley, K., Guthrie, E.H., Frost, S.R., 2011. Geometric morphometric analysis of tibial shape and presentation among Catarrhine taxa. Anat. Rec. 294, 217–230.
Tuttle, R.H., 1967. Knuckle-walking and the evolution of hominoid hands. Am. J. Phys. Anthropol. 26, 171–201.
Tuttle, R.H., 1969. Quantitative and functional studies on the hand of Anthropoidea. I. The Hominoidea. J. Morph. 128, 309–364.
Ward, C.V., Tocheri, M.W., Plavcan, J.M., Brown, F.H., Manthi, F.K., 2014. Early Pleistocene third metacarpal from Kenya and the evolution of modern human-like hand morphology. Proc. Natl. Acad. Sci. U. S. A. 111, 121–124.
Wiley, D.F., Amenta, N., Alcantara, D.A., Ghosh, D., Kil, Y.J., Delson, E., Harcourt-Smith, W., Rohlf, F.J., John, St., Hamann, K., Motani, B., Frost, R., Rosenbergerer, S., Tallman, A.L., Disotell, L., O'Neill, T.R., 2005. Evolutionary morphing. In: Visualization. VIS 05. IEEE, pp. 431–438.